FLOW CHARACTERISTICS OF SUPERSONIC LASER-SPIKE ENGINE

In-Seuck Jeung[*], Jeong-Yeol Choi[†], Sung-Don Kim[‡]

[*‡]Seoul National University, Seoul 151-744, Korea

[†]Pusan National University, Pusan 609-735, Korea

Abstract

Laser-spike engine is a promising candiadate as an inexpensive future launching system of small satellites into the space. In this paper, the flow characteristics and thrust generation mechanism in laser-spike engine were studied numerically and experimentally in the supersonic operation regime. First, two-dimensional Euler equation was applied to a linear laser-spike engine model. The initial 2-D model which was optically optimized showed the phenomenon of aerodynamic unstart process. Various phenomena could be observed varying experimental conditions. The conditions for regular start were investigated. Then axisymmetric models which have flat base and paraboloidal base were studied. Laser focusing points were changed according to geometries and applied laser energy was selected for cases of 1, 4, 10 and 40 Joules. The numerical simulations whthin supersonic operation regime based on the same laser energy input onto both base geometries show similar performance which is contrary to the experimental case. Detailed flow characteristics of laser-induced blast wave and thrust generation mechanism is discussed in detail.

Introduction

During the last decade, laser propulsion concept was studied by many investigators. Myrabo and Messitt succeeded to lift off a small body with a pulse type laser propulsion.[1] Recently, Sasoh suggested a laser-driven in-tube accelerator (LITA)[2], a concept of laser-propelled projectile in a barrel. Fig.1 shows a principle of it and laser-spike engine at supersonic velocity regimes.

Laser propulsion consist of using energy from a remotely located laser to heat propellant to extremely high temperature and pressure and then expand the gas or push projectile repetitively. Chemical rocket provides high thrust level and low overall weight but, specific impulse tends to be relatively low. Conversely, electric propulsion produces high specific impulse but low thrust level. Even nuclear engine has high thrust and high specific impulse, a massive nuclear reactor must be carried onboard. Instead of using energy from nuclear or chemical reactions to heat propellant, beamed laser energy is employed. This laser propulsion type device relies on high temperature pulse of repetitively breakdowned propellant to offer high specific impulse and high thrust. These can be grouped into two district categories depending on the type of laser used. One concept is to operate the laser in a steady-state mode known as continuous wave (CW) operation. The other is to use a repetitively pulsed (RP) laser which operates by producing high-frequency pulses of intense laser radiation.[1, 3]

This investigation treats laser-spike engine as one of the RP type laser-propulsion. In this concept, an incident laser light from a muzzle reflects at optically contoured projectile front area or directly on the

[*] Professor, Department of Aerospace Engineering, Seoul National University.
[†] Assistant Professor, Department of Aerospace Engineering, Pusan National University.
[‡] Graduate Student, Department of Aerospace Engineering, Seoul National University.

paraboloidal base area. At the focus of laser beams, propellant gas breaks down into plasma flow having core temperature of higher than 10,000K. Expansion of hot plasma flow gives an impact on the rear side of projectile remains at sufficiently high pressure for acceleration. Fig.1 show schematics of various laser-spike engine models considered in this paper.

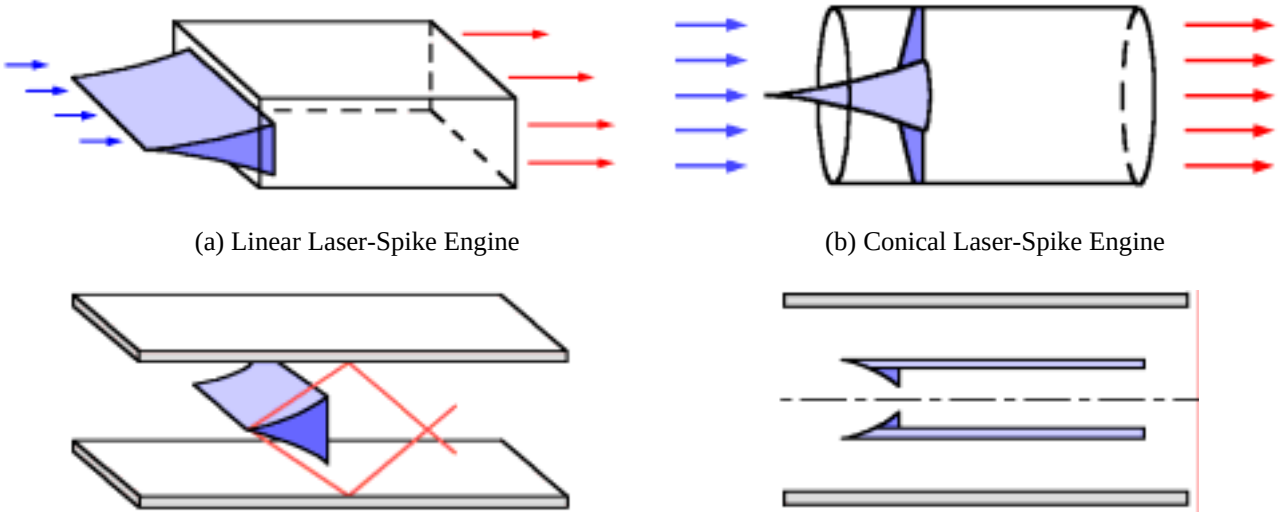

(a) Linear Laser-Spike Engine (b) Conical Laser-Spike Engine

(c) Linear LITA (d) Visualization Model in Wind Tunnel

Fig.1. Schematics of Laser-Spike Engines

The purpose of this paper is to examine the feasibility of laser-spike engine in the supersonic operation regime. This research treats laser focusing point locations, variable power sources, frequencies and projectile base geometries of the laser-spike engine for performance analysis assuming simplified energy source model. When the laser beam is introduced from the projectile front side and the projectile's base geometry is flat, we designate it as 'Flat base projectile'. And when the laser beam is introduced from the projectile rear side and the projectile's base geometry is parabolic, we will designate it as 'Paraboloidal base projectile' hereafter.

Experiment

The experimental study was conducted on the two-dimensional model shown in Fig.2. The surface contour of this model was based on that of Sasoh's axisymmetric projectile[4], but this model was divided into two parts in order to eliminate boundary layer effects which would be made by guiding tube when we installed an axisymmetric model. The scale factor of this model is 2.5 in comparison with Sasoh's one. So, the height between the upper plate and the lower one was 50mm, the length of contoured wedges was 41.75mm and the height 18.46mm.

These experiments were carried out in a supersonic wind tunnel in Seoul National University, which has the test section area of 200mm×200mm. The total pressure (p0) of settling chamber was maintained as 6.5kgf/cm2 (±2.5%) during experiments. The temperature showed a sharp fall because there was not an extra heat source to maintain constant temperature. Due to this reason, Reynolds number per unit length (Re/m) was also changed from 4.73×10^7 to 6.25×10^7. Though an experimental model was designed for the condition of optically optimized geometry, actual experiments were performed in Mach 3.0 condition.

In this study, shock structures were taken with Schlieren photography. The propagation of blast wave could also be detected by measuring at several surface points.

(a) Two-Dimensional Experimental Model (b) Installed Model in the Supersonic Wind Tunnel

Fig.2. Linear Laser-Spike Engine Model

Numerical Modeling

In this study, the viscous effects were assumed to be small since the propulsion mechanism is governed by dynamics of shock wave. Therefore, the Euler equations for two-dimensional and axisymmetric geometries were used as the governing equation of system with ideal gas assumption and heat addition term simmulating the laser focusing[5].

$$\frac{\partial \mathbf{Q}}{\partial t} + \frac{\partial \mathbf{F}}{\partial x} + \frac{\partial \mathbf{G}}{\partial y} + \alpha \mathbf{H} = \mathbf{W} \tag{1}$$

$$\boldsymbol{Q} = [\rho \quad \rho u \quad \rho v \quad e]^T \quad , \quad \boldsymbol{W} = [0 \quad 0 \quad 0 \quad q]^T \tag{2}$$

Since the propulsion process of LITA is governed by the unsteady propagation of blast wave, the numerical method to solve the governing equations should be highly accurate in space and time. Basicaly the finite volume method was used for the discretization of the governing equations in space. The Roe's approximate Riemann solver was used for the evaluation of numerical flexes at computational cell interfaces. The governing equation was integrated numerically with a second order time accurate implicit scheme (LU-SGS). An upwind-biased third-order MUSCL type TVD scheme was used for the spatial discretization of the invicid flux terms. Source energy term was calculated with explicit treatment. More detailed computational algorithm is addressed in the reference.[6] The inflow boundary condition was fixed and solid walls (projectile, tube) had slip line condition.

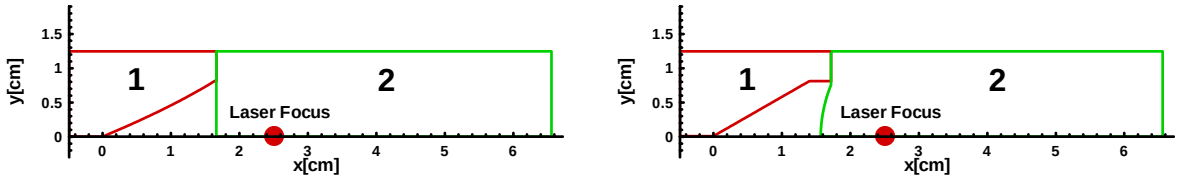

(a) Flat Base Projectile (b) Paraboloidal Base Projectile

Fig.3. Configurations used for Numerical Simulation

Numerical Validation

To evaluate the validity of numerical method used in this research, numerical results were compared with the experimental results conducted at Shock Wave Research Center, Institute of Fluid Science, Tohoku University. For details about the impulse and overpressure measurements, the reader should refer to Ref. 2. Fig.4 shows the experimental setup.

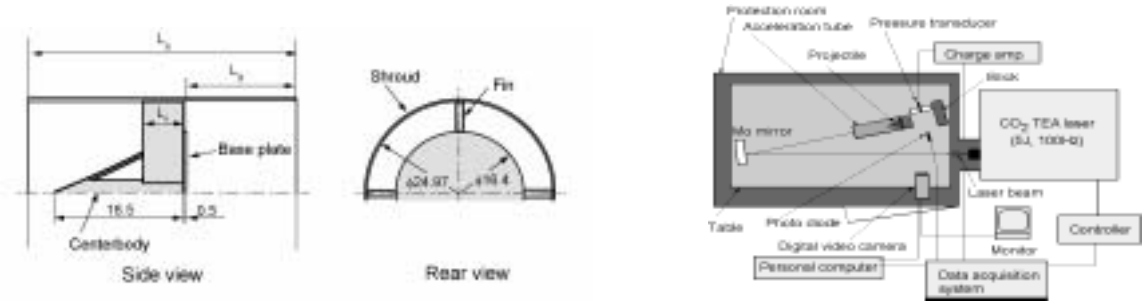

(a) Projectile Configuration, unit in mm. (b) Schematic of Experimental Apparatus

Fig.4. Experimental Setup

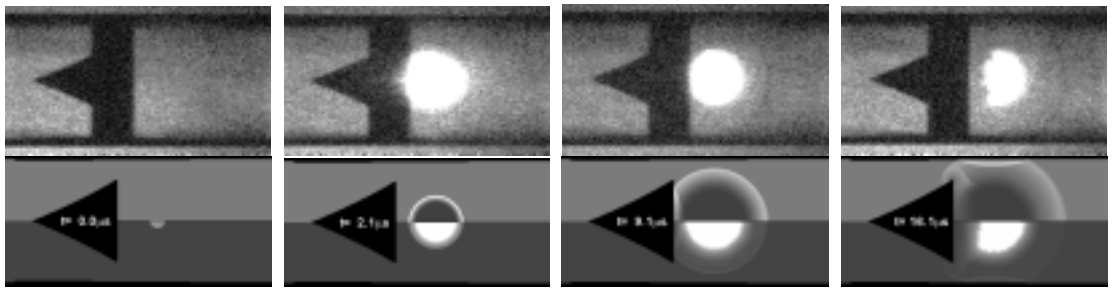

0.0 μs 2.1 μs 9.1 μs 16.1 μs

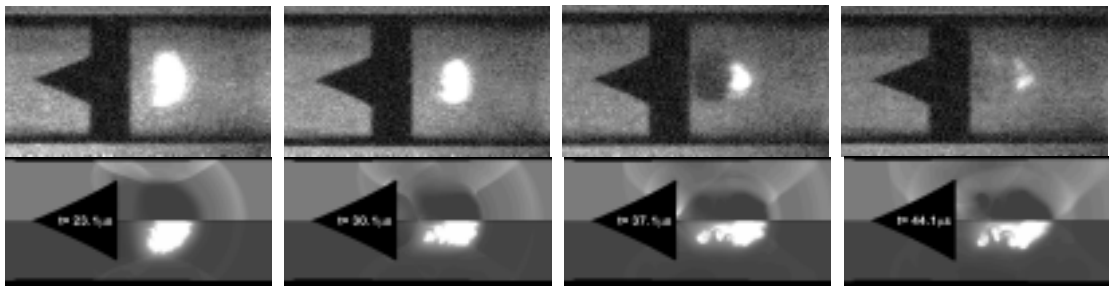

23.1 μs 30.1 μs 37.1 μs 44.1 μs

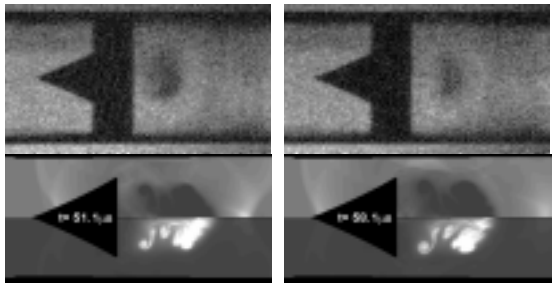

51.1 μs 58.1 μs

Fig.5. Framing Shadowgraph Images and Numerical Contour Plots showing Density (upper) and Temperature Field (lower).

The flow field after a laser beam irradiation is visualized using a high-speed framing camera (Imacon 200, DRS Hadland Ltd.) with shadowgraph arrangement. In order to view better the in-tube phenomena, an aspherical lens[8, 9] is used. Through the aspherical lens, the in-tube image is magnified vertically (normal to

the axis) by a factor of 2.06. The scaling in the axial direction remains unchanged. A xenon stroboflash is used as the light source. The framing shadowgraphs are shown in Fig.5 in comparison with numerical results.

Time interval between the experimental images is 7μs but the absolute time is ambiguous. So, times of the numerical results are selected with the fixed time interval, so that the location spherical shock wave in the third image (the clearest image showing the expanding spherical shock wave) agrees best. Projectile base is not shown in the experimental image since it is covered with the shroud designed for the reflection of laser beam. Even though the experimental visualization technique is the shadowgraph showing density field, temperature field is also plotted to represent the strong luminosity during the laser breakdown process.

The breakdown occurs at a moment between the frames 1 and 2. In comparison with numerical results, timing of frame 2 corresponds to 2.1μs. In this frame, an almost-spherical light-emission region is observed. Around this time, the hot gas core and a surrounding blast wave expand simultaneously. The bright region in numerical temperature contours correspond to the temperature higher than 10,000K.

In the third image at 9.1μs, a spherical hot core and a blast wave on its right-hand side are observed. Around this time the hot gas core finishes to expand and the blast wave decoupled from the hot gas region and expands continuously. The hot core corresponds to the plasma that is generated by directly absorbing the laser energy through bremsstralung. Being driven by the plasma core, the blast wave observed on the right configures almost a hemisphere. Although not shown in the shadowgraph images shaded by shroud, numerical image shows the reflected blast waves from the projectile base that is just before the interaction with the hot gas core.

In the next frame at 16.1μs, the blast wave is also visualized with an enlarged radius. However, the left side of the hot core is deformed. As seen in the numerical simulation, this deformation is caused by the reflected shock wave from the base of the centerbody. After reflection from the projectile base, diffraction to frontal area is observed at the corner. At the almost same moment, the incident blast wave reflects on the inner surface of shroud.

At 23.1μs, the reflected wave from the shroud interacts with the hot gas core and the acceleration of the wave front toward the axis of symmetry is observed due to a high speed of sound in the hot gas region. The accelerated shock wave reflects again at the axis of symmetry and a new wave emanates from the hot gas region, which expands to projectile surface and tube walls. The wave reflection is repeated periodically even though the wave strength decreases gradually. After 23.1μs, the region of the radiation emission is gradually shrunken; detailed flow/wave structure cannot be well resolved only in the experimental images.

From the above, it can be concluded that the numerical results showed quite a good agreement with the experiental data and proved valid.

Results

Linear Laser-Spike Engine

To know the characteristics for the various wedge geometry, Geometry Factor (GF) was defined. The GF for initial experimental geometry was defined as 1.0. To indicate the change of geometry, GF was multiplied to y coordinate values for wedge surface. Fig.6.(a) is the case of 0.75 GF which shows a result of normal start. Fig.6.(b) and (c) illustrates the change of flow according to the change of area ratio (AR). The case of AR=0.262 shows unstart result. In the case of 0.571, we can see the regular reflection and Mach reflection. This result indicates that the wedge angle of projectile is in condition of dual solution domain. In order to avoid the Mach reflection, Mach number should be changed. Fig.6.(d) is the case of Mach number 4.0 and AR=0.571 and shows only regular reflection.Fig.6.(e) shows the schlieren image of the case for AR=0.631. In this image, normal shock wave and expansion wave can be observed. The flow is choked in this case.

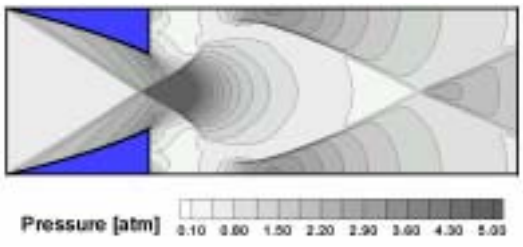

(a) M=3.0, AR=0.262, GF=0.75

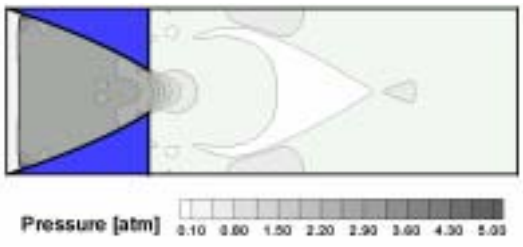

(b) M=3.0, AR=0.262, GF=1.0

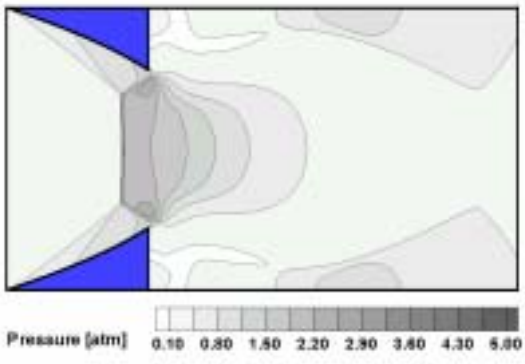

(c) M=3.0, AR=0.571, GF=1.0

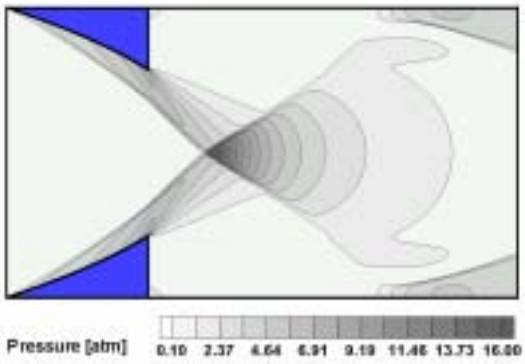

(d) M=4.0, AR=0.571, GF=1.0

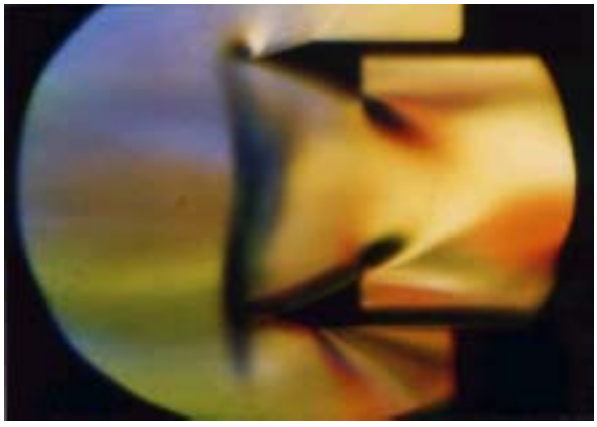

(e) M=3.0, AR=0.631, GF=1.0

Fig.6. Numerical and Experimental Results for Various Geometries

Axisymmetric Laser-Spike Engine

1. Flat Base Projectile

In flat base projectile, as a reference, incident laser beam is supplied from the projectile frontal side and reflects first on the specially contoured nose cone surface and secondly on the muzzle inner surface. This multiple reflection is considered by matching laser energy efficiency[7]. Fig.7 presents blast wave expansion according to time for a single pulsed laser focusing. This blast wave expansion and propagation was very

similar as previously observed case of very low subsonic propulsion[7].

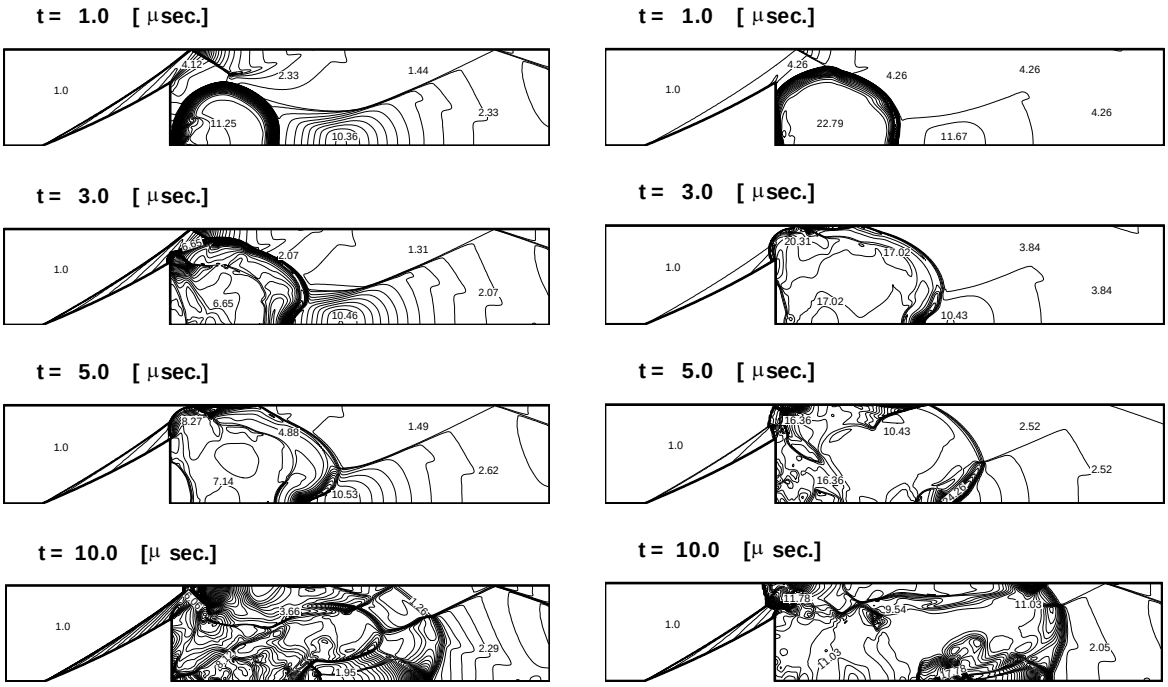

(a) Input Laser Power = 10J (b) Input Laser Power = 40J

Fig.7. Time Sequence of Pressure Contour Plots after Laser Focusing (Flat Base Projectile)

2. Paraboloidal Base Projectile

In paraboloidal base projectile, incident laser beam is supplied from the rear side of the projectile and reflected on the parabolic shaped base plate of the centerbody. Fig.8 presents blast wave expansion according to time under a single pulsed laser focusing.

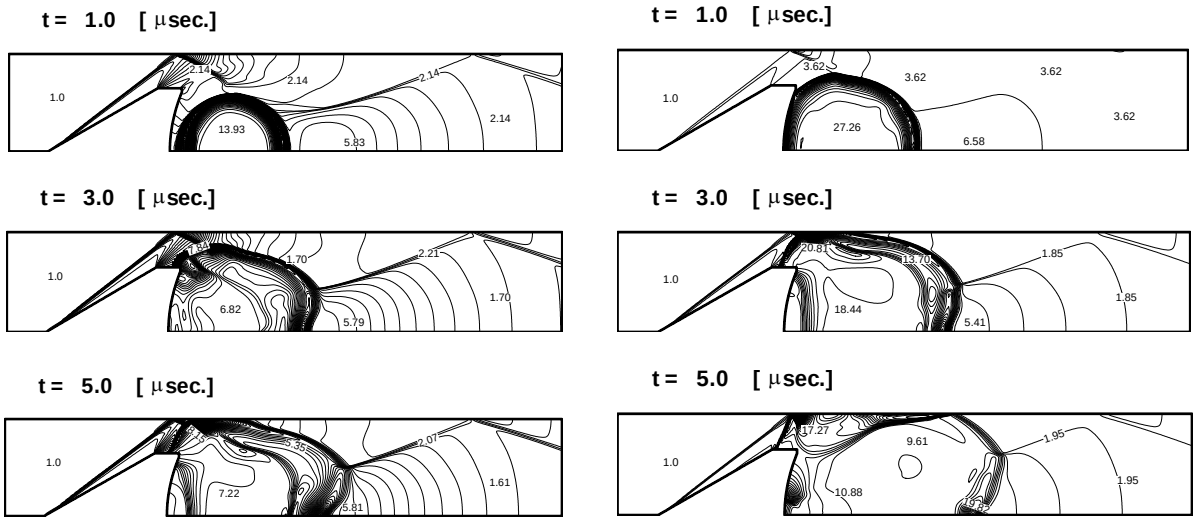

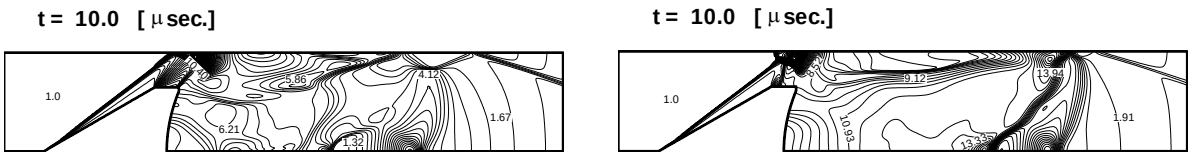

(a) Input Laser Power = 10J (b) Input Laser Power = 40J

Fig.8 Time Sequence of Pressure Contour Plots after Laser Focusing (Paraboloidal Base Projectile)

3. Comparison

When we compare the results of flat base projectile and paraboloidal base projectile, pressure wave propagation or thrust generation history was almost similar fashion in numerical simulation, significantly different from the previous experiment case. It would be due to the no modeling of the laser beam loss by the multiple reflections on the projectile surface in the case of flat base projectile, while less reflection in the case of paraboloidal base projectile. Fig.9 shows the time history of thrust.

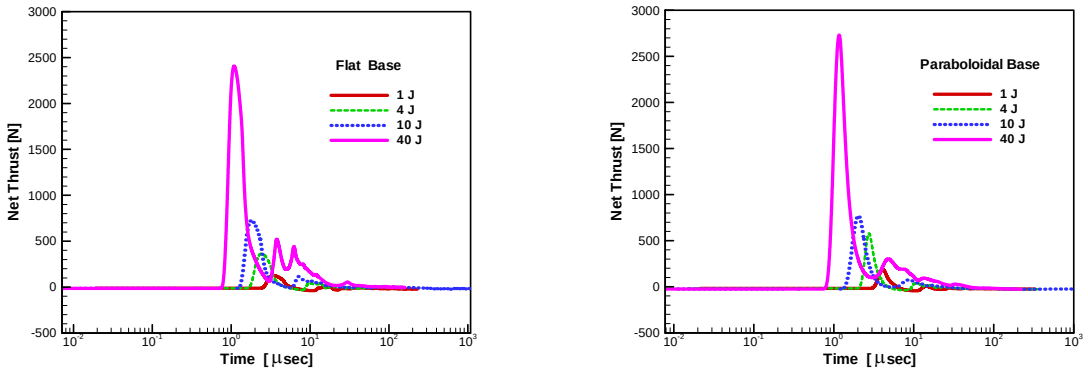

(a) Flat Base Projectile (b) Paraboloidal Base Projectile

Fig.9. Time History of Thrust

But aerodynamic drag induced by the projectile nose shape was noticed some difference of shock formation, or it would be noticeable to mention the effective influence of aerodynamic design rather than optical design optimization. Fig.10 shows the estimated coupling coefficient, C_m.

$$C_m = \frac{Cumulative \quad impulse}{One \quad pulse \quad laser \quad Energy}$$

In this calculation, cumulative impulse was selected as the time integral of the force increment from the aerodynamic drag. The coupling coefficient estimated in this calculation was fairly higher than the previous experiment[10] or numerical predictions.[10, 11] This would be probably due to (1) the modeling defects neglecting laser energy loss mechanisms such as plasma chemical reation and thermal radiation and (2) relatively lower input laser energy. In this calculation, energy conversion efficiency was selected as 33% for the case of flat base projectile[7], and 50% for the case of paraboloidal base projectile[11].

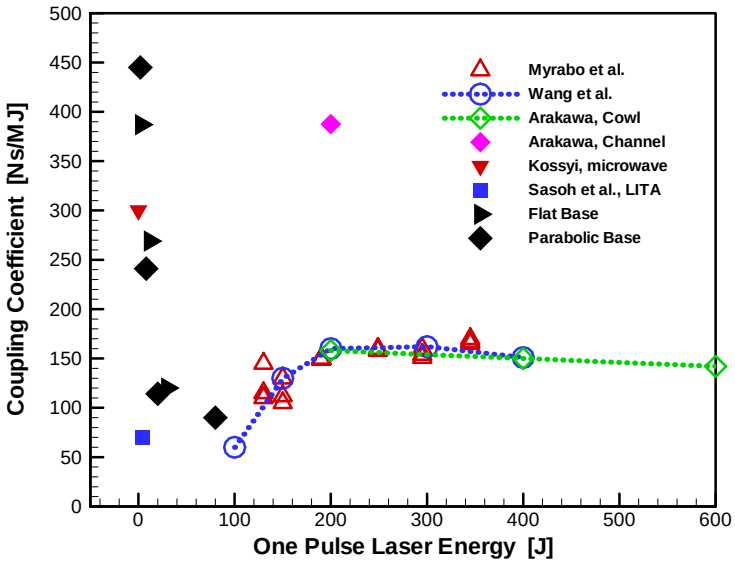

Fig.10. Estimated Coupling Coefficient

Conclusion

Numerical and experimental investigations on two-dimensional laser-spike engine model in supersonic condition were carried out. From the numerical results, the case of initial geometry showed an unstart process. In two-dimensional model, unstart processes happened easier than the axisymmetric model. In order to avoid unstart, increasing the area ratio can be a good solution, but Mach reflections are observed in any cases instead. Increasing Mach number or changing model geometry is required to solve the problem.

Axisymmetric laser-spike engine model's supersonic performance was numerically evaluated with simple thermal energy conversion concept. This result suggests that impulse generation mechanism of laser-spike engine would be mainly due to the supersonic blast wave. It is also noticeable to remark that laser energy loss mechanism should be included in the hyper speed performance evaluation, such as molecular breakdown process, light emission and radiation absorption process, and flux diffusion process etc. Definitions of coupling coefficient should be evaluated in the future for the better understandings of energy conversion. More extensive studies are expected on the operating conditions of laser-spike engine such as other flight Mach number and initial pressure condition.

Acknowledgement

Authors thank to Prof. A. Sasoh of Shock Wave Research Center, Tohoku University for providing information and experimental results. This study was partly supported by BK21 Program sponsored by Seoul National University.

References

[1] Myrabo, L. N. and Messitt, D. G., "Ground and Flight Test of a Laser Propelled Vehicle," AIAA 98-1001.
[2] Sasoh, A., "Laser-driven in-Tube Accelerator (LITA)," *Rev. Sci. Instrum.*, Vol.72, No.3, 2000.

[3] Birkan M. A., “Laser Propulsion: Status and Needs,” *Journal of Propulsion and Power*, Vol 8, No. 2, 1992, pp. 354-360.
[4] Sasoh, A., "In-Tube Laser Propulsin," AIAA 2000-2344
[5] Choi, J.-Y., Sasoh, A.,Jeung, I.-S.,Kim, S.-K., Cho, H.-J.,"Numerical and Experimental Studies of Laser-Driven Ram Accelerator," AIAA 2001-3924
[6] Choi, J.-Y., Jeung, I.-S. and Yoon, Y., “Computational Fluid Dynamics Algorithms for Unsteady Shock-Induced Combustion, Part 1: Validation,” *AIAA Journal*, Vol. 38, No. 7, July 2000, pp.1179-1187.
[7] Sasoh, A., Choi, J.-Y., Jeung, I.-S., Urabe. N., and Kleine. H., “Impulse Generation Mechanisms in Laser-driven In-Tube Accelerator,” submitted, *Journal of Propulsion and Power*, 2002
[8] Takayama, K. and Onodera, O., "Shock wave propagation past circular cross sectional 90 degree bend. Proc. 14th Int. Symp. On Shock Tube and Waves (Archer, R. D. and Milton, B. E. eds.), New South Wales Univ., Sydney, pp. 205-212.
[9] Sasoh, A. et al., "Diaphragm rupture. Impingement by a conically-nosed ram-accelerator projectile," Shock Waves, Vol. 9, 1999, pp. 19-30.
[10] Wang, T. S., Chen, Y. S., Liu, J., Myrabo, L. M., and Mead, F. B. Jr., “Advanced Performance Modeling of Experimental Laser Lightcraft”, *AIAA paper 2001-0648*, Jan., 2001
[11] Katsurayama, H., Komurasaki, K. and Arakawa, Y., “Numerical Analyses on Pressure Wave Propagation in Repetitive Pulse Laser Propulsion”, *AIAA paper 2001-3665*, July, 2000